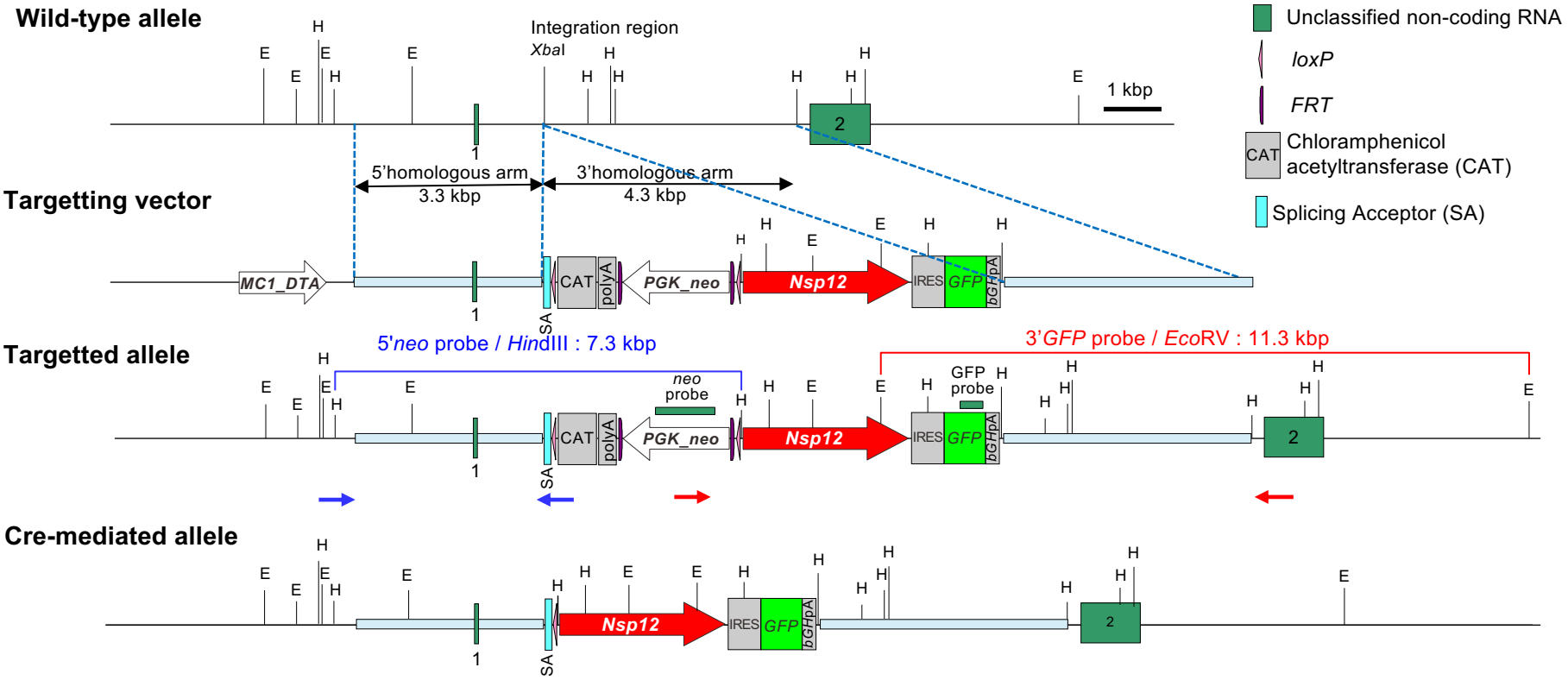

Extended Data Fig.1. Generation of the *Rosa26*-LSL-Nsp12 cKI mouse strain (Related to Fig.1a).

Targeting strategy for the construction of inducible SARS-CoV-2 Nsp12 knock-in mice (*Rosa26*-LSL-Nsp12$^{KI/-}$ mice; see Methods).
The PCR primers and Southern blot hybridization probes used to isolate homologous recombinants are shown as arrows and solid lines, respectively.
The *Hin*dIII fragment (7.3 kbp) hybridizable to the neo probe and the *Eco*RV fragment (11.3 kpb) hybridizable to the GFP probe are shown on the targeted allele. H, *Hin*dIII sites; E, *Eco*RV sites.

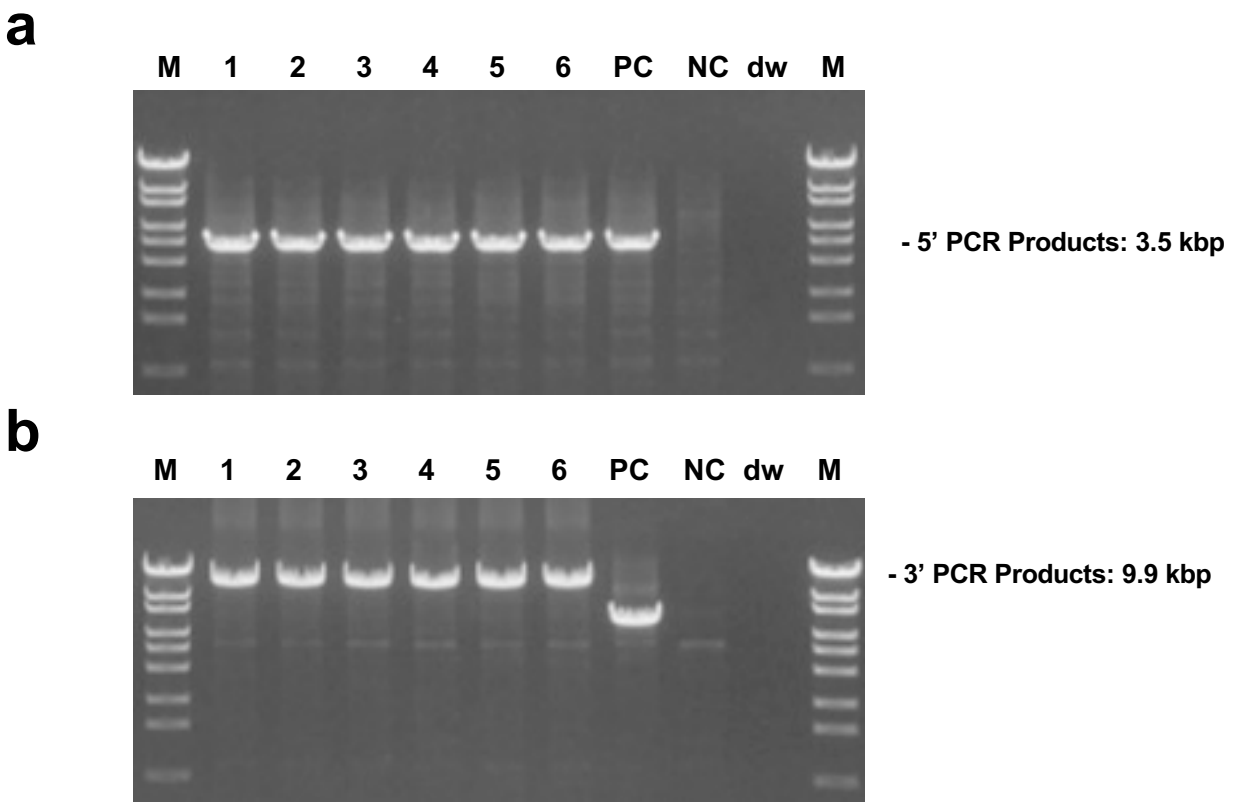

Extended Data Fig.2. PCR analysis to confirm homologous recombination in ES cells (Related to Fig.1a).
a, Confirmation of homologous recombination in ES cell clones by 5' PCR analysis.
Lanes 1-6, candidate ES cell clones; PC, previously obtained KI allele at the *ROSA26* locus (positive control);
NC, wild-type ES cells (negative control); dw, double-distilled water (negative control); M, λ/StyI size markers.
b, Confirmation of homologous recombination in the ES cell clones in (**a**) by 3' PCR analysis.

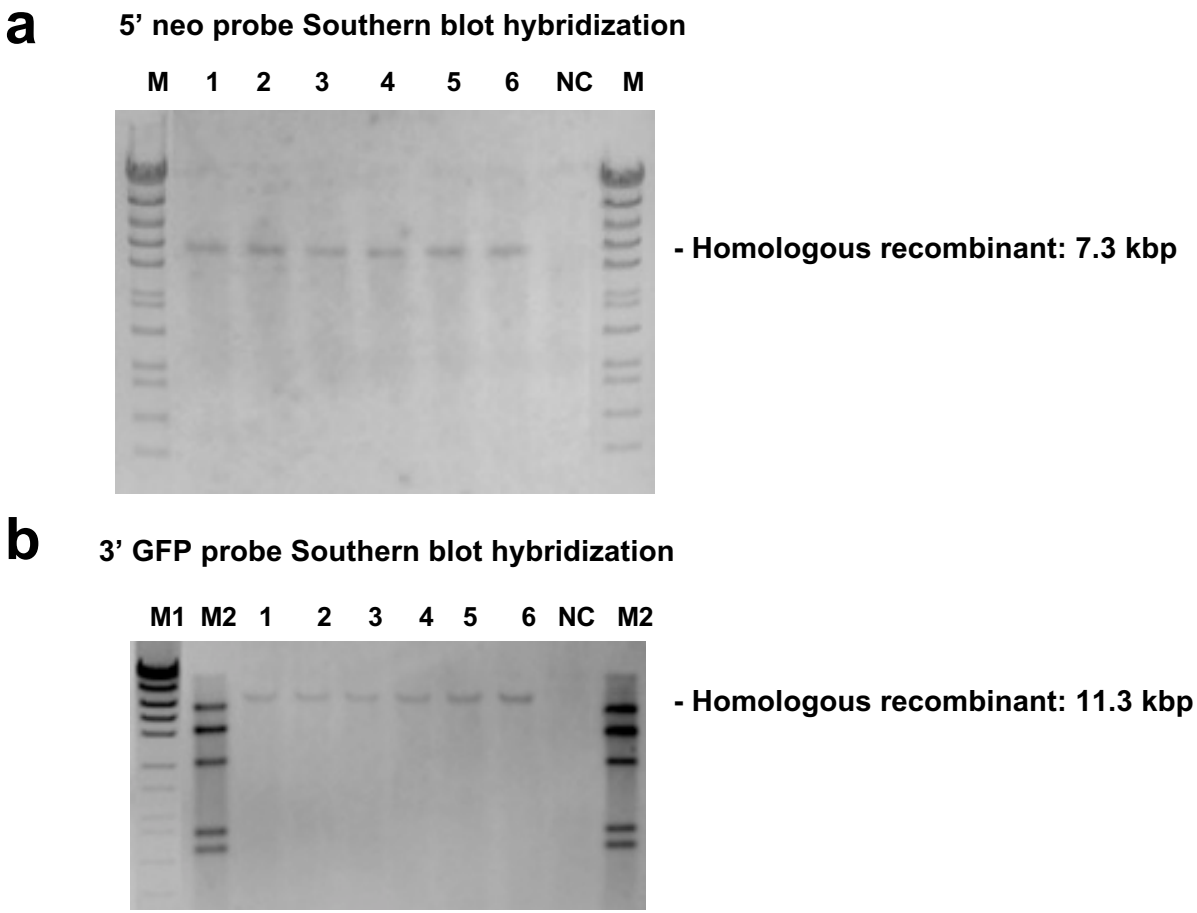

Extended Data Fig.3. Southern blot hybridization to confirm homologous recombination in ES cells (Related to Fig.1a).
a, Confirmation of homologous recombination in ES cell clones by 5’ genomic Southern blot hybridization with the neo probe.
Lanes 1-6, candidate ES cell clones; NC, wild-type ES cells (negative control); M, λ-*Eco*T14/*Bgl*II size markers.
b, Confirmation of homologous recombination in the ES cell clones in (**a**) by 3’ genomic Southern blot hybridization with the GFP probe.
Lanes 1-6, candidate ES cell clones; NC, wild-type ES cells (negative control); M1, λ-*Eco*T14/*Bgl*II size markers. M2, λ/*Hin*dIII size markers.

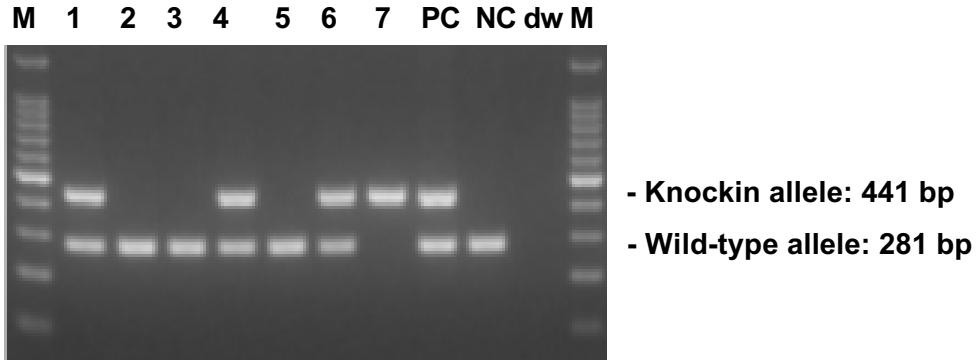

Extended Data Fig.4. PCR analysis of progeny from intercrossing of heterozygous *Rosa26*-LSL-Nsp12 cKI mice (Related to Fig. 1a).

Lanes 1-7, DNA of pups resulting from the intercrossing of heterozygous Rosa26-LSL-Nsp12$^{KI/-}$ mice; PC, heterozygous mouse (positive control); NC, wild-type mouse cells (negative control); dw, negative control; M, 100 bp ladder size markers.

Lanes 2, 3 and 5 show only the wild-type allele (281 bp amplified product), whereas lanes 1, 4 and 6 show heterozygosity for the knock-in allele (281 bp and 441 bp amplified products), and lane 7 is homozygous for the knock-in allele (441 bp amplified product).

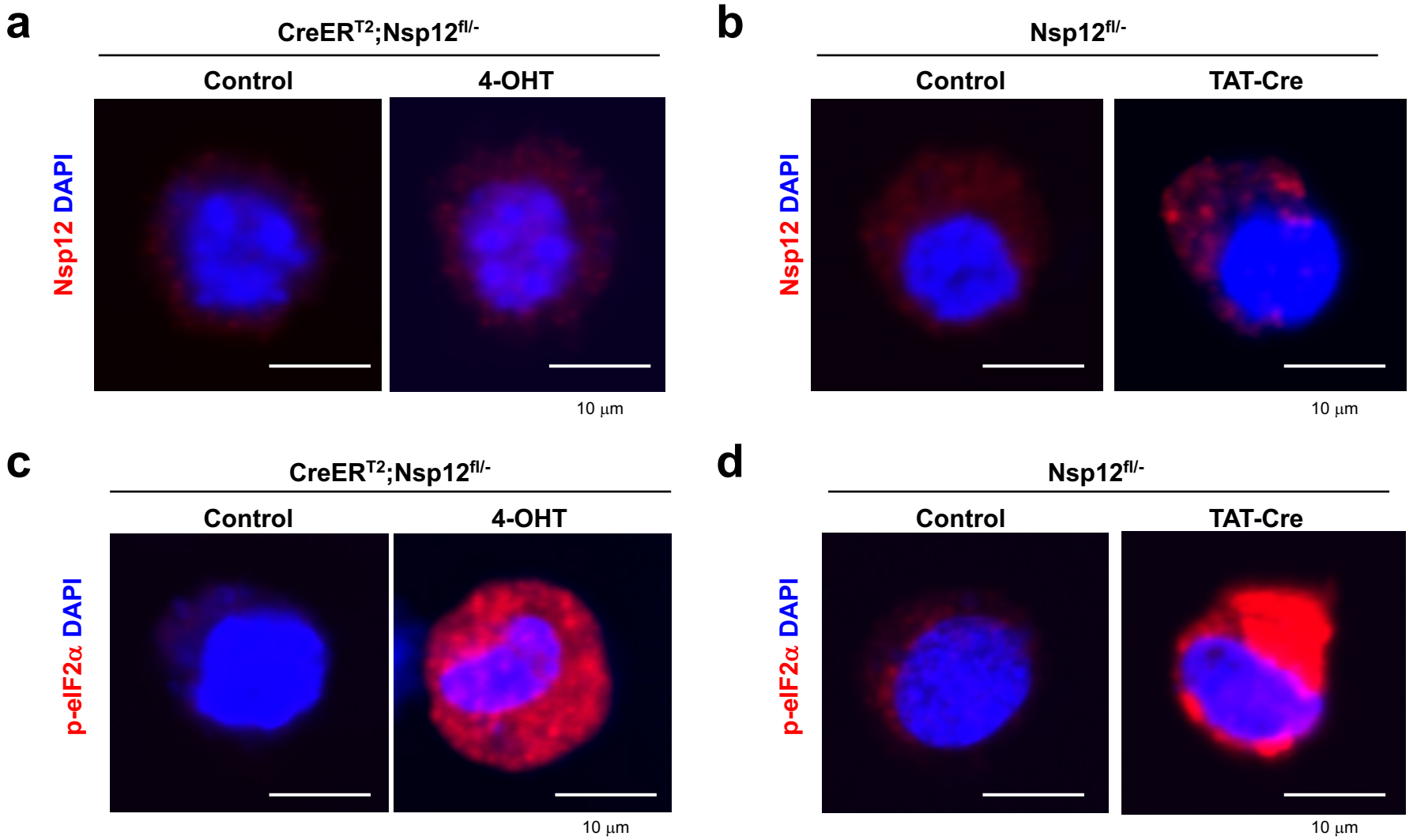

Extended Data Fig.5. Immunostaining to detect Nsp12 and phospho-eIF2α in primary lung epithelial cells of Nsp12 KI mice (Related to Fig.1b-d). **a-d,** Primary lung epithelial cells were isolated from (**a, c**) two male CreER^{T2};Nsp12$^{fl/-}$ mice (9-wk-old), or (**b, d**) two male Nsp12$^{fl/-}$ mice (9-wk-old). Cells were treated *in vitro* with (**a, c**) 4-OHT or (**b, d**) TAT-Cre. Cells were then immunostained with Abs to detect (**a, b**) Nsp12 or (**c, d**) phosphorylated eIF2α (Ser52). Nuclei were visualized using DAPI (blue). Results are representative of three biologically independent experiments.

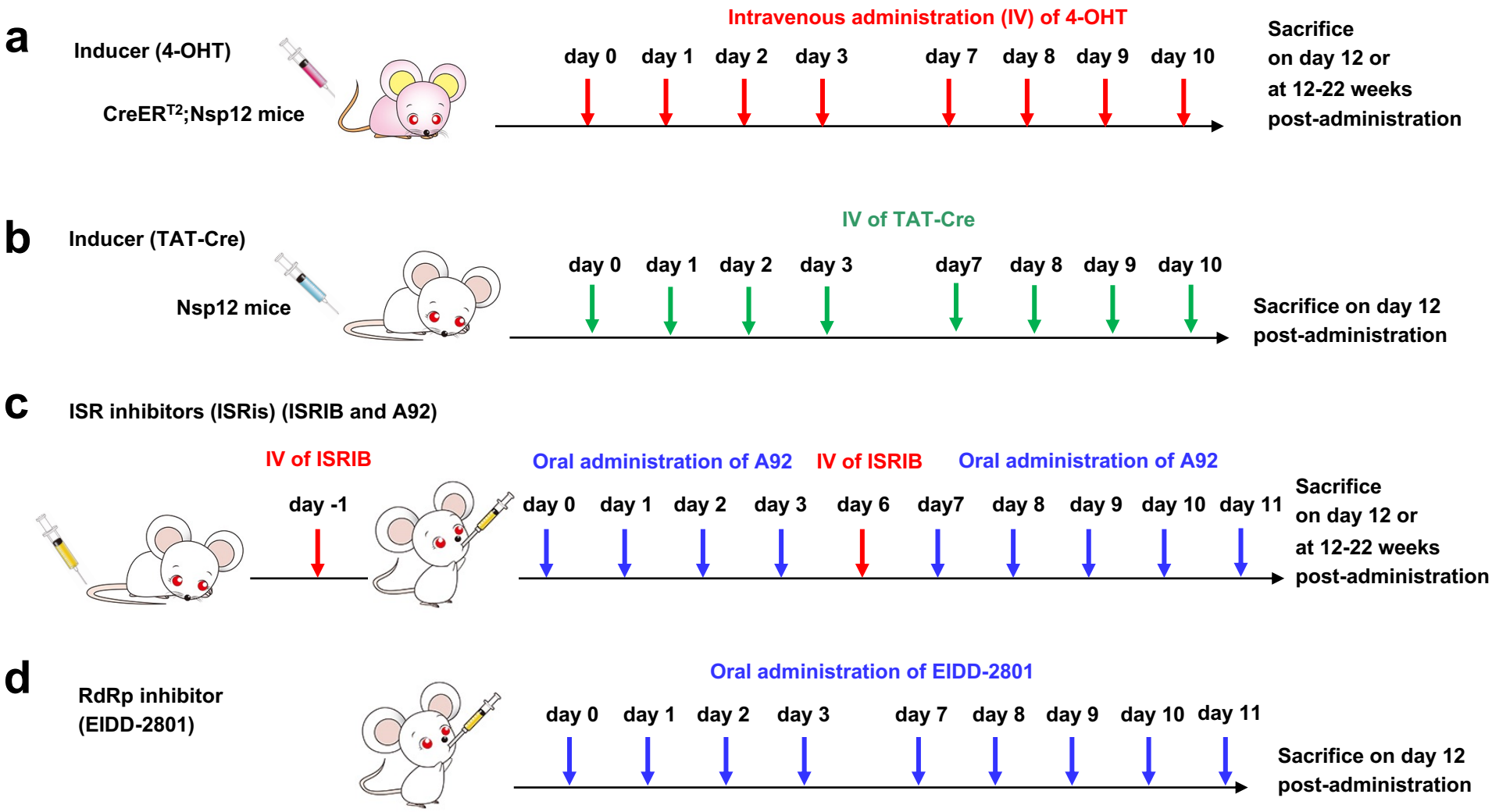

Extended Data Fig.6. *In vivo* treatment protocols of Nsp12 mouse strains.

a, To examine the *in vivo* effects of lung-specific expression of Nsp12, CreER^{T2};Nsp12 mice were intravenously injected with the inducer 4-OHT (5mg Kg^{-1}) on the indicated days. **b,** Nsp12 mice were intravenously injected with the inducer TAT-Cre recombinase (1,000 unit Kg^{-1}) on the indicated days. **c,** To examine the *in vivo* effects of ISR inhibitors (ISRis), CreER^{T2};Nsp12 mice and/or Nsp12 mice simultaneously underwent induction as in (a) or (b) and were intravenously injected with ISRIB (*Trans*-isomer) (5mg Kg^{-1}) on days -1 and 6, as indicated. Mice also received oral administration of A-92 (GCN2-IN-1, 0.4mg Kg^{-1}) in artificial gastric fluid as indicated. **d,** To examine the *in vivo* effects of an RdRp inhibitor, CreER^{T2};Nsp12 or Nsp12 mice simultaneously underwent induction as in (a) or (b) and (c) and received oral administration of EIDD-2801 (10mg Kg^{-1}) in artificial gastric fluid as indicated. Mice were sacrificed on day 12 or at the number of weeks post-administration indicated in the Figures, and tissue sections were acquired as described in Methods.

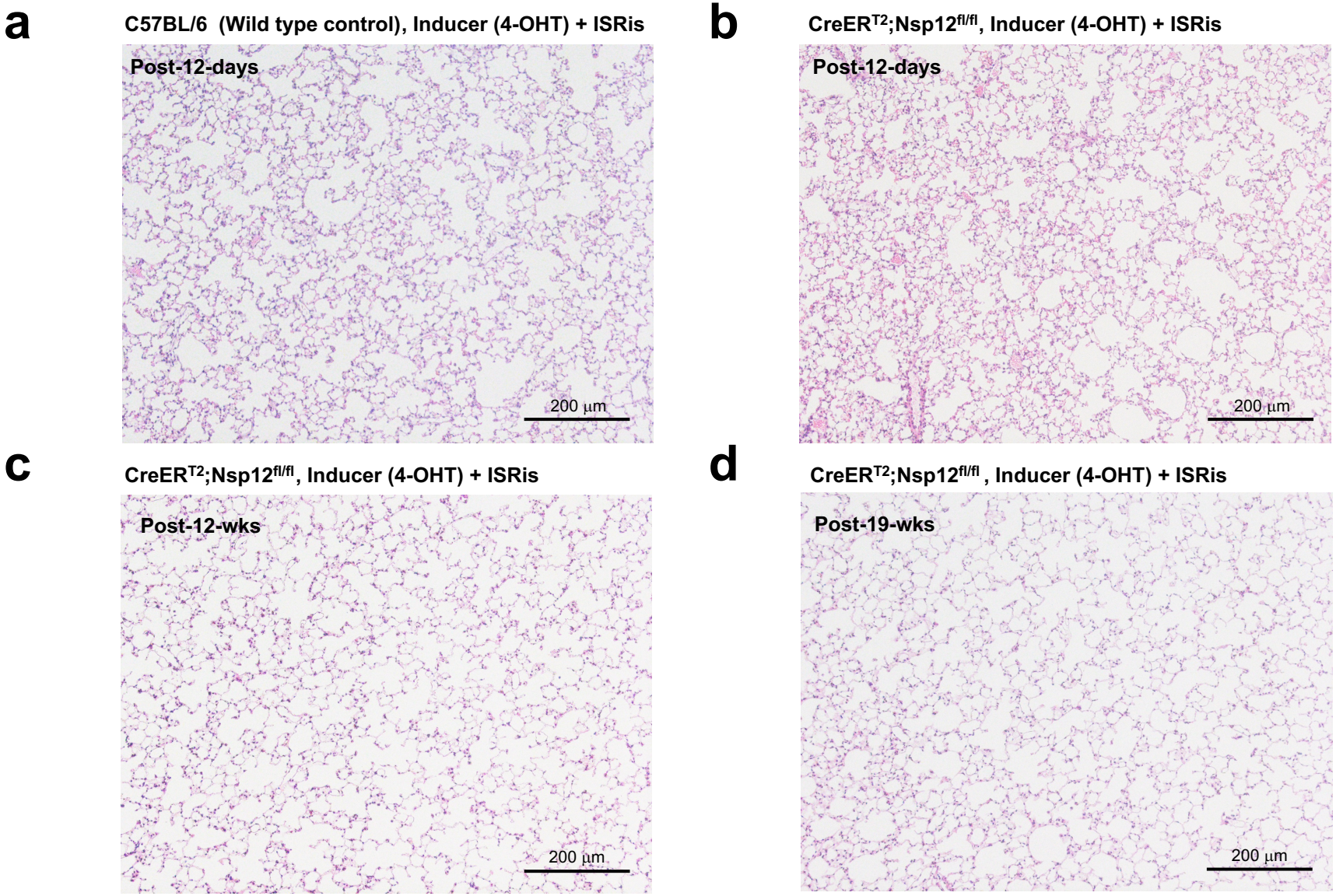

Extended Data Fig.7. SARS-CoV-2 Nsp12 does not induce pneumonia in Nsp12 mice.

a,b, Hematoxylin and Eosin (H&E) staining of lung tissues from **a)** one female C57BL/6 (wild-type control) mouse (5-wk-old), and **b)** one female CreER^{T2};Nsp12$^{fl/fl}$ mouse (5-wk-old) at 12 days after the start of *in vivo* treatment with 4-OHT+ISRis. **c,d,** H&E staining of lung tissues from **c)** one male CreER^{T2};Nsp12$^{fl/fl}$ mouse (16-wk-old) at 12 wks after the start of *in vivo* treatment with 4-OHT+ISRis, and **d)** one female CreER^{T2};Nsp12$^{fl/fl}$ mouse (24-wk-old) at 19 wks after the start of *in vivo* treatment with 4-OHT+ISRis. Results are representative of three biologically independent experiments.

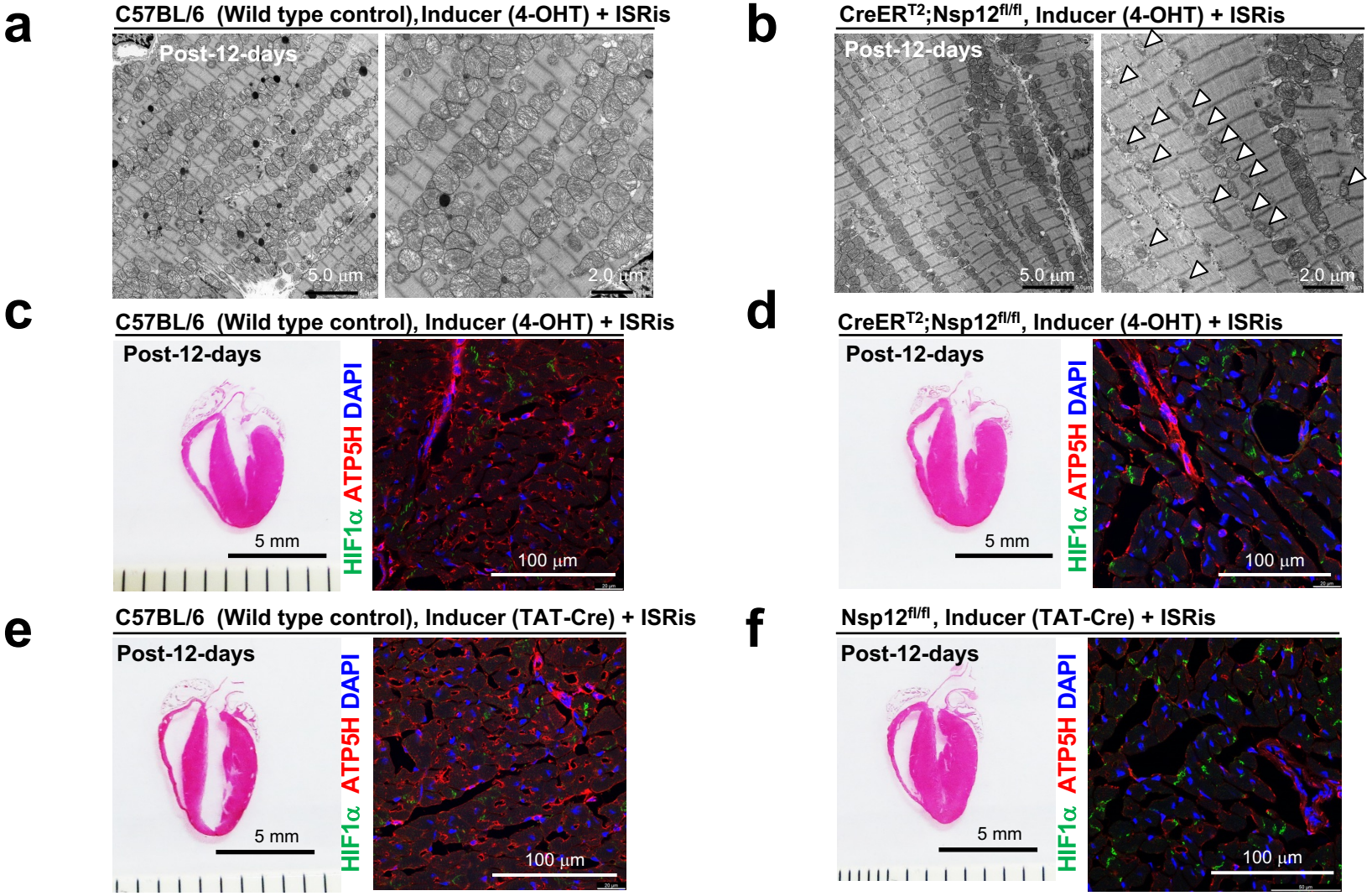

Extended Data Fig.8. Nsp12 expression in the lungs *in vivo* causes mitochondrial dysfunction in mouse heart in the short term (Related to Fig.3d,e). a,b, Representative transmission electron microscopy (TEM) images to detect mitochondrial ultrastructure and morphology in heart tissues of **a)** one female Nsp12$^{-/-}$ (C57BL/6 wild type control) mouse (8-wk-old) and **b)** one female CreER^{T2};Nsp12$^{fl/fl}$ mouse (6-wk-old) at 2 wks after the start of combined treatment with 4-OHT+ISRis (see Extended Data Fig.6a,c). White arrowheads indicate defective mitochondria without outer and inner membrane and/or cristae. **c-f,** Macroscopic views (left) and fluorescence co-immunostaining (right) to detect mouse anti-ATP5H Ab (red) and rabbit anti-HIF1α Ab (green) in frozen sections of heart tissues from **c)** one female Nsp12$^{-/-}$ (C57BL/6 wild type control) mouse (8-wk-old) and **d)** one female CreER^{T2};Nsp12$^{fl/fl}$ mouse (6-wk-old) at 12 days after the start of combined treatment with 4-OHT+ISRis (see Extended Data Fig.6a,c), and **e)** one female Nsp12$^{-/-}$ (C57BL/6 wild type control) mouse (8-wk-old) and **f)** one female Nsp12$^{fl/fl}$ mouse (6-wk-old) at 12 days after the start of combined treatment with TAT-Cre+ISRis (see Extended Data Fig.6b,c). DAPI, nuclei (blue). Results are representative of three biologically independent experiments.

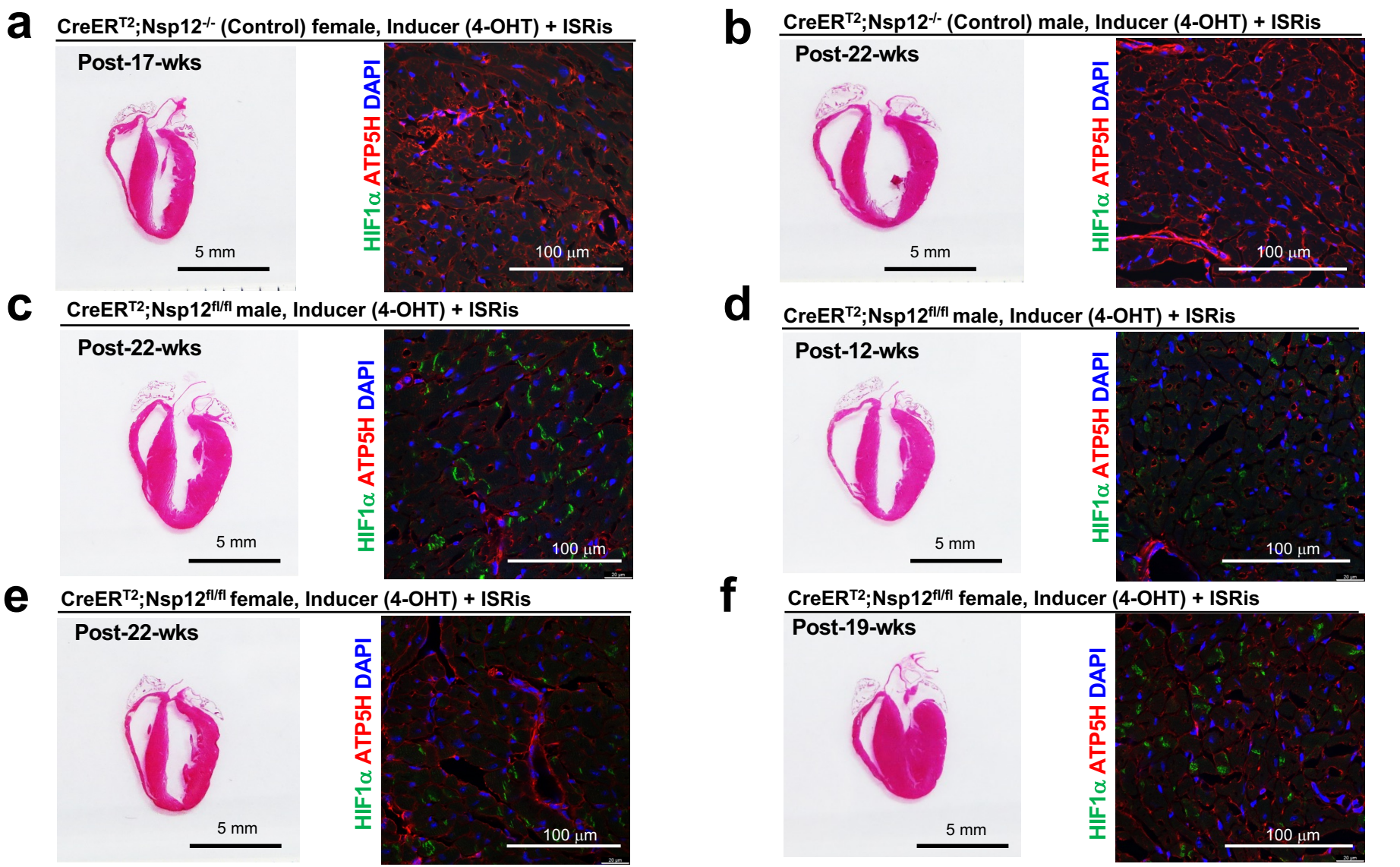

Extended Data Fig.9. Mitochondrial dysfunction in the hearts of Nsp12 cKI mice for the long term (Related to Fig.3f,g). a-f, Macroscopic views (left) and fluorescence co-immunostaining (right) to detect mouse anti-ATP5H Ab (red) and rabbit anti-HIF1α Ab (green) in frozen sections of heart tissues from **a)** one female CreER^{T2};Nsp12$^{-/-}$ (control) mouse (20-wk-old) at 17 wks after the start of 4-OHT+ISRis, **b)** one male CreER^{T2};Nsp12$^{-/-}$ (control) mice (25-wk-old) at 22 wks after the start of combined treatment with 4-OHT+ISRis; **c)** one male CreER^{T2};Nsp12$^{fl/fl}$ mouse (25-wk-old) at 22 wks after 4-OHT+ISRis; **d)** one male CreER^{T2};Nsp12$^{fl/fl}$ mouse (16-wk-old) at 12 wks after 4-OHT+ISRis; **e)** one female CreER^{T2};Nsp12$^{fl/fl}$ mouse (25-wk-old) at 22 wks after 4-OHT+ISRis; and **f)** one female CreER^{T2};Nsp12$^{fl/fl}$ mouse (23-wk-old) at 19 wks after 4-OHT+ISRis (see Extended Data Fig.6a,c). DAPI, nuclei (blue).